www.ietdl.org

Published in IET Communications
Received on 24th June 2012
Revised on 17th August 2012
doi: 10.1049/iet-com.2012.0355

ISSN 1751-8628

Super-orthogonal trellis-coded spatial modulation

E. Başar[1] *Ü. Aygölü*[1] *E. Panayırcı*[2] *H.V. Poor*[3]

[1]*Faculty of Electrical and Electronics Engineering, Istanbul Technical University, 34469 Maslak, Istanbul, Turkey*
[2]*Department of Electronics Engineering, Kadir Has University, 34083 Cibali, Istanbul, Turkey*
[3]*Department of Electrical Engineering, Princeton University, Princeton, NJ 08544, USA*
E-mail: basarer@itu.edu.tr

Abstract: Spatial modulation (SM), which employs the indices of multiple transmit antennas to transmit information in addition to the conventional M-ary signal constellations, is a novel transmission technique that has been proposed for multiple-input multiple-output systems. In this study, a new class of space-time trellis codes, called 'super-orthogonal trellis-coded SM' (SOTC-SM), is proposed. These codes combine set partitioning and a super set of space-time block coded SM (STBC-SM) codewords to achieve maximal diversity and coding gains by exploiting both SM and space-time block codes. Unlike super-orthogonal space-time trellis codes (SOSTTCs), which parametrise the orthogonal STBCs, these new codes expand the antenna constellation using the principle of SM. Systematic construction methods are presented for the SOTC-SM scheme and design examples are given for 2, 4 and 8 trellis states, at 2, 3 and 4 bits/s/Hz spectral efficiencies. The approximate bit-error probability performance of SOTC-SM is derived and shown to match computer simulation results. A simplified maximum likelihood detection method for the proposed scheme is given. It is shown through computer simulations that the proposed SOTC-SM schemes achieve significantly better error performance than SOSTTCs with comparable complexity.

Nomenclature

Bold, lowercase and capital letters	used for column vectors and matrices, respectively
$(.)^*$, $(.)^T$ and $(.)^H$	complex conjugation, transposition and Hermitian transposition, respectively
$\|\| \cdot \|\|$	Euclidean (or Frobenius) norm
$\Pr(\cdot)$	probability of an event
$\det(\boldsymbol{A})$ and $\text{rank}(\boldsymbol{A})$	determinant and rank of $\boldsymbol{A}$, respectively
$\mathcal{R}\{x\}$	real part of x for a complex variable x
$Q(\cdot)$	tail probability of the standard Gaussian distribution

1 Introduction

Spatial multiplexing systems such as the vertical Bell Labs layered space-time (V-BLAST) system [1] boost the data rate by the simultaneous transmission of a group of information symbols, where each antenna transmits its own data. On the other hand, space-time block codes (STBCs) have been designed to increase the reliability of transmission by means of transmit diversity [2, 3]. STBCs have been comprehensively studied in the literature because of their ability to exploit the promising potential of multiple-input multiple-output (MIMO) systems effectively. However, to obtain additional coding gains without expanding the bandwidth, space-time trellis codes (STTCs), which combine modulation and trellis coding for MIMO systems, have been proposed [4]. Therefore STTCs can be considered as trellis-coded modulation (TCM) schemes [5] for MIMO channels. On the other hand, it has been shown in [6, 7] that a systematically designed class of STTCs, called super-orthogonal STTCs (SOSTTCs), can achieve higher coding gains than classical STTCs with lower decoding complexity by combining the STBCs with trellis codes, applying the set partitioning principle to the STBC matrices and super-orthogonal sets.

The fundamental feature of SM, which makes it different from the conventional MIMO techniques, is the use of the antenna indices as a source of information in addition to the conventional M-ary signal constellations such as M-ary phase-shift keying (M-PSK) or M-ary quadrature amplitude modulation (M-QAM) [8]. SM features some interesting properties such as the elimination of inter-channel interference and no requirement of antenna synchronisation as well as reduction of the required number of radio frequency (RF) chains to one at the transmitter. By eliminating amplitude/phase modulations for SM, a space-shift keying (SSK) scheme [9] has been proposed and extensively studied [10]. Recently, improved SM and SSK schemes have been proposed [11–13]. In order to improve the error performance of SM, a novel scheme called space-time block-coded spatial modulation (STBC-SM) has been proposed in [14] by combining SM with STBC to benefit from the diversity gain advantage of

STBC. In this scheme, the information is conveyed by not only STBC matrices, but also by the indices of the transmit antennas over which the matrices are transmitted. A suboptimal trellis-coded SM scheme, which benefits from the trellis coding gain for SM under correlated channel conditions, has been proposed in [15], where the key idea of TCM is partially applied to SM. More recently, a new spatial modulation for trellis coding (SM-TC) scheme has been proposed in [16], in which a trellis encoder and an SM mapper are jointly designed, similarly to the conventional TCM. This scheme does not permit parallel transitions in order to maintain the same time diversity advantage of the trellis coding as the classical STTCs. It has been shown in [16] that the SM-TC achieves significantly better bit-error rate (BER) and frame error rate (FER) performance than the STTCs with reduced decoding complexity, since only one transmit antenna is active during each trellis transition. However, for SM-TC schemes, the required number of transmit antennas must be an integer power of 2, and spectral efficiencies such as 3 and 4 bits/s/Hz can be achieved with eight transmit antennas, which significantly increase their implementation complexity. Furthermore, no method for designing reliable SM-TC codes systematically has yet been discovered.

In this paper, a new class of STTCs, called 'super-orthogonal trellis-coded spatial modulation (SOTC-SM)', is proposed. In this scheme, using the principle of set partitioning for STBC-SM matrices, STBC-SM is combined with trellis coding, and systematic techniques are presented for designing new trellis codes with 2, 4 and 8 trellis states at 2, 3 and 4 bits/s/Hz spectral efficiencies. Compared to SM-TC, the proposed codes do not restrict the number of transmit antennas and they can also be designed systematically. The proposed codes not only allow simplified decoding as SOSTTCs do, but also do not expand the signal constellation. Unlike the classical SOSTTCs, which parametrise the orthogonal STBCs to obtain the required number of orthogonal matrices to be assigned to the branches of the trellis, we expand the antenna constellation using the principle of SM. Although the proposed codes have the same minimum coding gain distances (CGDs), determined by the 'parallel transitions', as those of SOSTTCs, the expansion to the antenna domain improves the 'distance spectrum' of SOSM-TC schemes significantly. This results in an improved error performance since the diversity order of our scheme exceeds that of the core STBC for the 'error events with higher lengths' [7]. The pairwise error probability (PEP) of the proposed SOTC-SM scheme and an approximate bit-error probability (BEP) expression is derived. A simplified maximum-likelihood (ML) detection technique for SOTC-SM is presented and its computational complexity is evaluated. It is shown through computer simulations that the proposed codes achieve significantly better BER and FER performance than the SOSTTCs and the SM-TC schemes, with comparable complexity.

The organisation of the paper is as follows. In Section 2, we introduce the SOTC-SM scheme, given the corresponding construction techniques and provide several design examples. In Section 3, the error performance analysis for SOTC-SM is presented. In Section 4, a simplified ML decoding technique for SOTC-SM is investigated. In Section 5, simulation results and performance comparisons are given. Finally, in Section 6, the main conclusions of the paper are presented.

2 Super-orthogonal trellis coded spatial modulation

In this section, we first briefly review the STBC-SM technique and present the set partitioning principle for STBC-SM matrices. We then introduce the proposed SOTC-SM scheme with specific design examples for different trellis states and spectral efficiencies.

2.1 STBC-SM and super set of STBC-SM codewords

The STBC-SM technique presented in [14] combines STBCs with SM to improve the overall transmission efficiency by means of spatial diversity and coding gain. As an example, using Alamouti's STBC, the STBC-SM provides the following codeword set for three transmit antennas

$$\left\{ \boldsymbol{X}^a = \begin{bmatrix} x_1 & x_2 & 0 \\ -x_2^* & x_1^* & 0 \end{bmatrix}, \quad \boldsymbol{X}^b = \begin{bmatrix} 0 & x_1 & x_2 \\ 0 & -x_2^* & x_1^* \end{bmatrix} \right\} \tag{1}$$

where x_1 and x_2 are two complex information symbols drawn from an M-PSK or M-QAM signal constellation and the columns and rows correspond to the transmit antennas and the symbol intervals, respectively. In this work, we call the codeword set in (1) a 'super set' [7] of STBC-SM codewords for three transmit antennas. The codeword set in (1) is obtained by the extension of Alamouti's STBC to three transmit antennas and doubles the number of orthogonal matrices provided by a single codeword in (1). This property of STBC-SM is the main motivation of our work. As will be seen shortly, the super sets of STBC-SM codewords will be used at the trellis transitions of the proposed SOTC-SM scheme.

2.2 Construction of the SOTC-SM scheme

We now systematically explain how to design the new STTCs using SM, which we call the SOTC-SM, for a given spectral efficiency (κ bits/s/Hz) and an arbitrary number of states (S). The SOTC-SM technique is based on the set partitioning of the STBC-SM codewords for a given signal constellation format. The key point in set partitioning of an orthogonal STBC-SM codeword $\boldsymbol{X}$ is to find subsets such as $\boldsymbol{X}_i$, $\boldsymbol{X}_{ij}$ or $\boldsymbol{X}_{ijk}$, $i, j, k \in \{1, 2\}$ of its realisation matrices, with progressively larger minimum CGDs [7]. The minimum CGD is an important design parameter for quasi-static Rayleigh fading channels, for which the channel fading coefficients remain constant during the transmission of a frame. By considering all possible realisations $\boldsymbol{C}^i$ and $\boldsymbol{C}^j$ of an STBC-SM codeword $\boldsymbol{X}$, the minimum CGD for this codeword is defined as

$$\delta_{\min} = \min_{\boldsymbol{C}^i, \boldsymbol{C}^j} \det(\boldsymbol{C}^i - \boldsymbol{C}^j)^{\mathrm{H}} (\boldsymbol{C}^i - \boldsymbol{C}^j) \tag{2}$$

For SOTC-SM, we apply the set partitioning for each STBC-SM codeword in a considered codeword set as in (1). Let us assume quadrature PSK (QPSK), 8-PSK and 16-QAM constellations with the codeword $\boldsymbol{X}^a$ in (1). The orthogonal matrices provided by this codeword can be partitioned into eight subsets as shown in Fig. 1, where because of space limitations, the corresponding pairs of symbol indices are provided for QPSK and 8-PSK constellations only, for which the index of the constellation symbol $e^{j(2\pi/M)(a-1)}$ is denoted by $a \in \{1, 2, \ldots, M\}$. However, using a similar

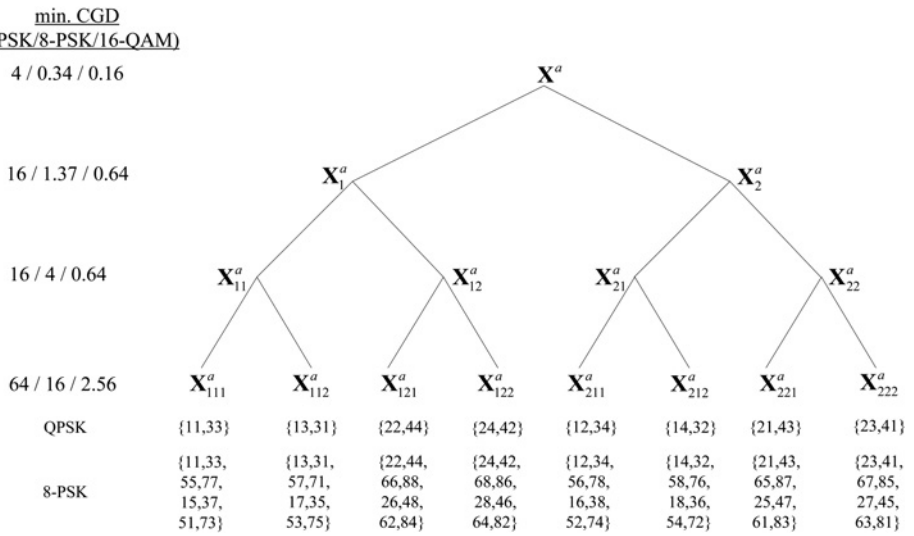

Fig. 1 *Set partitioning of the STBC-SM codewords for QPSK, 8-PSK and 16-QAM constellations and the corresponding pairs of symbol indices for QPSK and 8-PSK, only*

technique, set partitioning can be performed for other constellations. As shown on the left-hand side of Fig. 1, the minimum CGD increases as we move down to the lower levels of the tree. Note that the set partitioning given for $\boldsymbol{X}^a$ in Fig. 1 is valid for other STBC-SM codewords employing different antenna combinations.

During the SOTC-SM construction, we assign different STBC-SM codewords to the transitions originating from different states, which not only guarantees the transmit diversity of the corresponding STBC, but also avoids a catastrophic encoder. Furthermore, when compared with the classical SOSTTCs, the use of the antenna domain improves the distance spectrum of the trellis code significantly, resulting in a substantial improvement in error performance while maintaining the same spectral efficiency and trellis structure. In other words, SOSTTCs use a super set of STBCs whereas our scheme uses a super set of STBC-SM codewords, where both schemes apply set partitioning to their corresponding sets to achieve full-diversity with maximum coding gain. SOSTTCs expand the number of orthogonal matrices without expanding the signal constellation, which is a desired feature for simplified transmitter structure. Contrary to the STBC-SM technique, the SOTC-SM also has this feature, which expands the antenna constellation rather than parametrising the code like the SOSTTCs do.

For κ bits/s/Hz, we have $2^{\kappa T}$ branches diverging from each state when a $T \times n_T$ STBC is employed, where T and n_T denote the number of channel uses and the number of transmit antennas, respectively. In particular for the case of Alamouti's STBC, we have $2^{2\kappa}$ branches diverging from a state. For SOTC-SM, we employ two different trellis code construction techniques, as follows.

1. We assign a different STBC-SM codeword to each state of the trellis, and therefore S different STBC-SM codewords are required. This approach resembles that used for the SOSTTCs, in which a different rotation parameter is assigned to each state. Contrary to the SOSTTCs, we extend the orthogonal matrices in the spatial domain rather than the parameter domain. For the branches diverging from each state, we apply the set partitioning rules explained above to obtain the corresponding subsets.

2. $S/2$ STBC-SM codewords are employed and their subsets are arranged systematically when assigning to the branches diverging from different states to avoid a catastrophic encoder. A similar design technique has also been reported for SOSTTCs.

For both of the construction techniques described above, where a total of $2^{2\kappa}S$ orthogonal matrices are assigned to the branches of the trellis for the Alamouti code, a rate-1 code is obtained, that is, $\kappa = \log_2(M)$. As we will show in the sequel, although similar techniques as those of SOSTTCs are applied, extending the core STBC to the spatial domain rather than the parameter domain provides significant advantages in terms of the error performance and provides design flexibility with interesting trade-offs between complexity and performance. Furthermore, it overcomes the limitation of classical SOSTTCs for which the total number of required orthogonal matrices is limited by the number of different rotation parameters, which do not expand the signal constellation.

2.3 New trellis code design examples

In this subsection, we provide several code design examples for 2, 3 and 4 bits/s/Hz spectral efficiencies and different numbers of trellis states using the aforementioned trellis code construction techniques employing the Alamouti code in STBC-SM codewords. The number of considered transmit antennas varies from three to six depending on the chosen trellis structure and the construction technique. Owing to space limitations, trellis diagrams of the new codes are defined by the subsets assigned to the state transitions, represented by $S \times S$ state transition matrices as shown in Table 1, where the submatrix at the ith row and jth column, $i, j = 1, \ldots, S$ represents the subset assigned to the parallel transitions diverging from the ith state and merging to the jth state. A zero matrix $\mathbf{0}$ means that there is no transition between the corresponding two states, and $\boldsymbol{X}^a$, $\boldsymbol{X}^b$, $\ldots$, $\boldsymbol{X}^h$ represent the STBC-SM codewords with different antenna combinations, which will be given in the sequel. As an example, the trellis diagram of the 4-state SOTC-SM scheme is given in Fig. 2, where its corresponding subsets can be verified from Table 1. We now present the new code constructions, as follows.

doi: 10.1049/iet-com.2012.0355

Table 1 Trellis state transition matrices for SOTC-SM schemes with subsets assigned to parallel transitions

State	Matrix
2	$\begin{bmatrix} X_1^a & X_2^a \\ X_1^b & X_2^b \end{bmatrix}$
4	$\begin{bmatrix} X_{11}^a & X_{12}^a & X_{21}^a & X_{22}^a \\ X_{11}^b & X_{12}^b & X_{21}^b & X_{22}^b \\ X_{11}^c & X_{12}^c & X_{21}^c & X_{22}^c \\ X_{11}^d & X_{12}^d & X_{21}^d & X_{22}^d \end{bmatrix}$
8-I	$\begin{bmatrix} X_{11}^a & X_{12}^a & X_{21}^a & X_{22}^a & 0 & 0 & 0 & 0 \\ 0 & 0 & 0 & 0 & X_{11}^b & X_{12}^b & X_{21}^b & X_{22}^b \\ X_{11}^c & X_{12}^c & X_{21}^c & X_{22}^c & 0 & 0 & 0 & 0 \\ 0 & 0 & 0 & 0 & X_{11}^d & X_{12}^d & X_{21}^d & X_{22}^d \\ X_{21}^a & X_{22}^a & X_{11}^a & X_{12}^a & 0 & 0 & 0 & 0 \\ 0 & 0 & 0 & 0 & X_{21}^b & X_{22}^b & X_{11}^b & X_{12}^b \\ X_{21}^c & X_{22}^c & X_{11}^c & X_{12}^c & 0 & 0 & 0 & 0 \\ 0 & 0 & 0 & 0 & X_{21}^d & X_{22}^d & X_{11}^d & X_{12}^d \end{bmatrix}$
8-II 8-III	$\begin{bmatrix} X_{111}^a & X_{112}^a & X_{121}^a & X_{122}^a & X_{211}^a & X_{212}^a & X_{221}^a & X_{222}^a \\ X_{111}^b & X_{112}^b & X_{121}^b & X_{122}^b & X_{211}^b & X_{212}^b & X_{221}^b & X_{222}^b \\ X_{111}^c & X_{112}^c & X_{121}^c & X_{122}^c & X_{211}^c & X_{212}^c & X_{221}^c & X_{222}^c \\ X_{111}^d & X_{112}^d & X_{121}^d & X_{122}^d & X_{211}^d & X_{212}^d & X_{221}^d & X_{222}^d \\ X_{111}^e & X_{112}^e & X_{121}^e & X_{122}^e & X_{211}^e & X_{212}^e & X_{221}^e & X_{222}^e \\ X_{111}^f & X_{112}^f & X_{121}^f & X_{122}^f & X_{211}^f & X_{212}^f & X_{221}^f & X_{222}^f \\ X_{111}^g & X_{112}^g & X_{121}^g & X_{122}^g & X_{211}^g & X_{212}^g & X_{221}^g & X_{222}^g \\ X_{111}^h & X_{112}^h & X_{121}^h & X_{122}^h & X_{211}^h & X_{212}^h & X_{221}^h & X_{222}^h \end{bmatrix}$

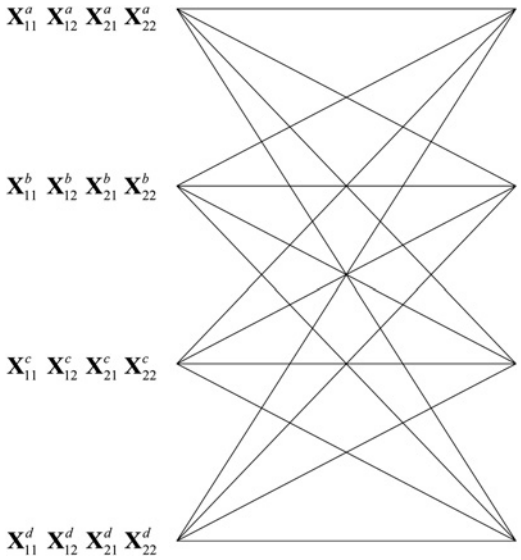

Fig. 2 *New four-state SOST-SM scheme using QPSK for 2 bits/s/Hz or 8-PSK for 3 bits/s/Hz or 16-QAM for 4 bits/s/Hz*

2.3.1 Example 2.1, (2-state): For a 2-state code, the two codewords of (1) are assigned to the states of the trellis according to the first construction technique as seen from Table 1. In order to obtain spectral efficiencies of 2, 3 and 4 bits/s/Hz, we use QPSK, 8-PSK and 16-QAM modulations for which the corresponding minimum CGDs are equal to 16, 1.37 and 0.64, respectively. Note that the minimum CGD of our 2-state SOTC-SM scheme is the same as that of the 2-state SOSTTC. Although the worst case PEP events for our code and the 2-state SOSTTC are the same and are determined by the parallel transitions, extending the code in the spatial domain improves the distance spectrum of the trellis code significantly, by means of the error events with higher lengths. We will examine the PEP behaviour of this code in the next section.

2.3.2 Example 2.2 (4-state): Fig. 2 demonstrates the proposed 4-state trellis code constructed by the first technique using the corresponding set partitioning as well as the following STBC-SM codewords for four transmit antennas

$$\boldsymbol{X}^a = \begin{bmatrix} x_1 & x_2 & 0 & 0 \\ -x_2^* & x_1^* & 0 & 0 \end{bmatrix} \quad \boldsymbol{X}^b = \begin{bmatrix} 0 & x_1 & x_2 & 0 \\ 0 & -x_2^* & x_1^* & 0 \end{bmatrix}$$
$$\boldsymbol{X}^c = \begin{bmatrix} 0 & 0 & x_1 & x_2 \\ 0 & 0 & -x_2^* & x_1^* \end{bmatrix} \quad \boldsymbol{X}^d = \begin{bmatrix} x_1 & 0 & 0 & x_2 \\ -x_2^* & 0 & 0 & x_1^* \end{bmatrix} \tag{3}$$

Although having the same minimum CGD as that of our previous 2-state code for QPSK and 16-QAM constellations, this code has a better distance spectrum because of its reduced number of parallel transitions. Note that the minimum CGD of this code for 8-PSK is equal to 4, which is higher than that of the code in Example 2.1. Four STBC-SM codewords with four transmit antennas were used here to obtain the required number of orthogonal matrices in Fig. 2.

2.3.3 Example 2.3 (8-state-I): The four codewords of (3) are assigned to the branches of the trellis according to the second construction technique as seen from Table 1. For QPSK, 8-PSK and 16-QAM modulations, the minimum CGD of this code is the same as that of the 4-state code given in Example 2.2. However, when compared with the codes in Examples 2.1 and 2.2, this code exhibits better error performance because of its increased trellis complexity, which improves the distance spectrum. Note that a similar 8-state SOSTTC is also reported in [7] with the same minimum CGD for 8-PSK.

2.3.4 Example 2.4 (8-state-II): As seen from Table 1, the second 8-state trellis code is constructed by the first technique using the following eight STBC-SM codewords for five transmit antennas

$$\boldsymbol{X}^a = \begin{bmatrix} x_1 & x_2 & 0 & 0 & 0 \\ -x_2^* & x_1^* & 0 & 0 & 0 \end{bmatrix} \quad \boldsymbol{X}^b = \begin{bmatrix} 0 & 0 & x_1 & x_2 & 0 \\ 0 & 0 & -x_2^* & x_1^* & 0 \end{bmatrix}$$
$$\boldsymbol{X}^c = \begin{bmatrix} 0 & x_1 & x_2 & 0 & 0 \\ 0 & -x_2^* & x_1^* & 0 & 0 \end{bmatrix} \quad \boldsymbol{X}^d = \begin{bmatrix} x_1 & 0 & 0 & 0 & x_2 \\ -x_2^* & 0 & 0 & 0 & x_1^* \end{bmatrix}$$
$$\boldsymbol{X}^e = \begin{bmatrix} x_1 & 0 & x_2 & 0 & 0 \\ -x_2^* & 0 & x_1^* & 0 & 0 \end{bmatrix} \quad \boldsymbol{X}^f = \begin{bmatrix} 0 & x_1 & 0 & x_2 & 0 \\ 0 & -x_2^* & 0 & x_1^* & 0 \end{bmatrix}$$
$$\boldsymbol{X}^g = \begin{bmatrix} x_1 & 0 & 0 & x_2 & 0 \\ -x_2^* & 0 & 0 & x_1^* & 0 \end{bmatrix} \quad \boldsymbol{X}^h = \begin{bmatrix} 0 & 0 & x_1 & 0 & x_2 \\ 0 & 0 & -x_2^* & 0 & x_1^* \end{bmatrix} \tag{4}$$

The minimum CGD values of this code are equal to 64, 16 and 2.56 for QPSK, 8-PSK and 16-QAM, respectively, which are higher than those of the code in the previous example, because of the reduced number of parallel transitions. In order to obtain $8M^2$ matrices for $\kappa = \log_2(M)$ bits/s/Hz, a total of eight transmit antenna combinations are

required, that can be supported by at least five transmit antennas according to the STBC-SM design technique [14].

2.3.5 Example 2.5 (8-state-III): This code has the same structure and minimum CGD values as those of our 8-state-II code; however, it uses the following STBC-SM codewords for six transmit antennas

$$\boldsymbol{X}^a=\begin{bmatrix} x_1 & x_2 & 0 & 0 & 0 & 0 \\ -x_2^* & x_1^* & 0 & 0 & 0 & 0 \end{bmatrix} \quad \boldsymbol{X}^b=\begin{bmatrix} 0 & 0 & x_1 & x_2 & 0 & 0 \\ 0 & 0 & -x_2^* & x_1^* & 0 & 0 \end{bmatrix}$$

$$\boldsymbol{X}^c=\begin{bmatrix} 0 & 0 & 0 & 0 & x_1 & x_2 \\ 0 & 0 & 0 & 0 & -x_2^* & x_1^* \end{bmatrix} \quad \boldsymbol{X}^d=\begin{bmatrix} 0 & x_1 & x_2 & 0 & 0 & 0 \\ 0 & -x_2^* & x_1^* & 0 & 0 & 0 \end{bmatrix}$$

$$\boldsymbol{X}^e=\begin{bmatrix} 0 & 0 & 0 & x_1 & x_2 & 0 \\ 0 & 0 & 0 & -x_2^* & x_1^* & 0 \end{bmatrix} \quad \boldsymbol{X}^f=\begin{bmatrix} x_1 & 0 & 0 & 0 & 0 & x_2 \\ -x_2^* & 0 & 0 & 0 & 0 & x_1^* \end{bmatrix}$$

$$\boldsymbol{X}^g=\begin{bmatrix} x_1 & 0 & x_2 & 0 & 0 & 0 \\ -x_2^* & 0 & x_1^* & 0 & 0 & 0 \end{bmatrix} \quad \boldsymbol{X}^h=\begin{bmatrix} 0 & x_1 & 0 & x_2 & 0 & 0 \\ 0 & -x_2^* & 0 & x_1^* & 0 & 0 \end{bmatrix} \tag{5}$$

which improves the distance spectrum further to obtain better error performance.

3 Performance evaluation of SOTC-SM

In this section, we first derive the PEP expressions for the most dominant error events. We then obtain a closed-form approximation to the average BEP by considering the PEP of the error events with lengths up to a given finite value. We are restricted to this approximation of the average BEP since the evaluation of a true union bound using the transfer function is not feasible for the considered MIMO quasi-static fading channel model.

Suppose that the Alamouti code is considered. For the STBCs and STTCs, let us assume that a $2N \times n_T$-dimensional code matrix $\boldsymbol{X}$ is transmitted and erroneously detected as $\hat{\boldsymbol{X}}$, where N is the error event path length. Note that for the STBCs, $N = 1$. The conditional PEP is given by the following well-known formula [7]

$$\Pr(\boldsymbol{X} \to \hat{\boldsymbol{X}}|\boldsymbol{H}) = Q\left(\sqrt{\frac{\gamma}{2}}\|(\boldsymbol{X}-\hat{\boldsymbol{X}})\boldsymbol{H}\|\right) \tag{6}$$

where γ is the average SNR at each receive antenna, assuming the average power of the received signal at each receive antenna is 1 W, $\boldsymbol{H}$ is the $n_T \times n_R$ fading channel coefficient matrix with zero mean, unit variance circularly symmetric complex Gaussian distributed entries, where n_R denotes the number of receive antennas. Averaging (6) over $\boldsymbol{H}$ and using moment-generating function (MGF) techniques, the unconditional PEP is given as [17]

$$\Pr(\boldsymbol{X} \to \hat{\boldsymbol{X}}) = \frac{1}{\pi}\int_0^{\pi/2}\prod_{i=1}^{r}\left(\frac{\sin^2\theta}{\sin^2\theta+(\gamma/4)\lambda_i}\right)^{n_R} \mathrm{d}\theta \tag{7}$$

where λ_i $(i = 1, 2, \ldots, r)$ and r are the ith eigenvalue and the rank of the distance matrix $A(\boldsymbol{X}, \hat{\boldsymbol{X}}) = (\boldsymbol{X}-\hat{\boldsymbol{X}})^H(\boldsymbol{X}-\hat{\boldsymbol{X}})$, respectively. A closed-form expression for (7) is given in ([17], eq. (5A.74)). After the evaluation of the PEP, the approximate BEP performance of the SOTC-SM scheme is calculated by considering error events with lengths up to a predetermined finite value as [17]

$$P_b \simeq \frac{1}{n}\sum_{\boldsymbol{X}}\left[\frac{1}{\kappa'}\sum_{\substack{\hat{\boldsymbol{X}} \\ \hat{\boldsymbol{X}}\neq\boldsymbol{X}}} e(\boldsymbol{X}, \hat{\boldsymbol{X}})\Pr(\boldsymbol{X} \to \hat{\boldsymbol{X}})\right] \tag{8}$$

where κ' is the number of input bits per trellis transition (i.e. $\kappa' = 2\kappa$ for the case where the Alamouti code is used on the branches of the trellis), n is the total number of different transmission matrices and $e(\boldsymbol{X}, \hat{\boldsymbol{X}})$ is the number of bit errors associated with the corresponding error event. In the following, we give a generic example to show the accuracy of (8) for our scheme, considering all possible values of $\boldsymbol{X}$ and $\hat{\boldsymbol{X}}$ matrices for error events with lengths $N = 1$ (parallel transitions) and 2. As we show in the sequel, our assumptions are quite efficient, since the theoretical curves match closely with Monte Carlo simulation results, and therefore there is no need to consider error events with higher lengths, which can be quite complicated for some trellis codes.

3.1 Example 3.1 (2 bits/s/Hz, 2-state)

For the parallel transitions of the new 2-state code, the PEP expression in (7) reduces to the PEP of the Alamouti's STBC, which is given by

$$\Pr(\boldsymbol{X} \to \hat{\boldsymbol{X}}) = \frac{1}{\pi}\int_0^{\pi/2}\left(\frac{\sin^2\theta}{\sin^2\theta+(\gamma/4)\lambda}\right)^{2n_R} \mathrm{d}\theta \tag{9}$$

where $\lambda_1 = \lambda_2 = \lambda$ because of the orthogonality of the Alamouti code. The approximate BEP performance of our scheme can be calculated easily from (8) as

$$P_b \simeq \frac{1}{32}\left[\sum_{\boldsymbol{X}_1^a}\sum_{\hat{\boldsymbol{X}}_1^a}\Pr(\boldsymbol{X}_1^a \to \hat{\boldsymbol{X}}_1^a)e(\boldsymbol{X}_1^a, \hat{\boldsymbol{X}}_1^a)\right] \tag{10}$$

where because of the symmetrical code design, we have considered error events only within the parallel transitions originating from the first state and merging to the first state (for the sake of notational simplicity, we use $\boldsymbol{X}_1^a$ for both a subset and its elements). Numerical analysis of the approximation given by (10) is exactly the same as that for a 2-state SOSTTC [7] and shows that a transmit diversity order of two is achieved for both schemes. On the other hand, extending the core STBC to the antenna domain allows higher transmit diversity orders than that of the core STBC itself for the case $N \geq 2$. We obtain $2 < r \leq n_T$ with increasing N and, consequently, the superiority of the proposed scheme becomes more evident.

As an example, for $N = 2$, considering the error event path pairs originating from the first state, we have two cases for which $\boldsymbol{X} = \left[(\boldsymbol{X}_1^a(1))^T \quad (\boldsymbol{X}_1^a(2))^T\right]^T$, $\hat{\boldsymbol{X}} = \left[(\boldsymbol{X}_2^a(1))^T \quad (\boldsymbol{X}_1^b(2))^T\right]^T$ and $\boldsymbol{X} = \left[(\boldsymbol{X}_1^a(1))^T \quad (\boldsymbol{X}_2^a(2))^T\right]^T$, $\hat{\boldsymbol{X}} = \left[(\boldsymbol{X}_2^a(1))^T \quad (\boldsymbol{X}_2^b(2))^T\right]^T$, respectively, where $\boldsymbol{X}_i^m(t)$, $m \in \{a, b\}$ and $i = 1,2$ denotes the transmission of $\boldsymbol{X}_i^m$ in the tth step $(t = 1, \ldots, N)$ of the

doi: 10.1049/iet-com.2012.0355

error event. For these cases, we have

$$\boldsymbol{X} = \begin{bmatrix} x_{1,1} & x_{2,1} & 0 \\ -x_{2,1}^{*} & x_{1,1}^{*} & 0 \\ x_{1,2} & x_{2,2} & 0 \\ -x_{2,2}^{*} & x_{1,2}^{*} & 0 \end{bmatrix}$$

$$\hat{\boldsymbol{X}} = \begin{bmatrix} \hat{x}_{1,1} & \hat{x}_{2,1} & 0 \\ -\hat{x}_{2,1}^{*} & \hat{x}_{1,1}^{*} & 0 \\ 0 & \hat{x}_{1,2} & \hat{x}_{2,2} \\ 0 & -\hat{x}_{2,2}^{*} & \hat{x}_{1,2}^{*} \end{bmatrix} \tag{11}$$

where $x_{i,t}$ and $\hat{x}_{i,t}$ are the ith data symbols in the tth transmitted and erroneously detected STBC-SM matrices along the error event, respectively. The use of a third transmit antenna with the SM principle allows a transmit diversity order of three for $\boldsymbol{X}$ and $\hat{\boldsymbol{X}}$ matrices in (11), which can be proved by showing that $\delta = \mathrm{CGD} = \det A(\boldsymbol{X}, \hat{\boldsymbol{X}})$ is non-zero for all values of $\boldsymbol{X}$ and $\hat{\boldsymbol{X}}$. After some algebra, it follows from (11) that

$$\begin{aligned} \delta = {} & (|\hat{x}_{1,2}|^2 + |\hat{x}_{2,2}|^2)(|x_{1,1} - \hat{x}_{1,1}|^2 \\ & + |x_{2,1} - \hat{x}_{2,1}|^2)(|x_{1,1} - \hat{x}_{1,1}|^2 \\ & + |x_{2,1} - \hat{x}_{2,1}|^2 + |x_{1,2} + \hat{x}_{2,2}|^2 + |\hat{x}_{1,2} - x_{2,2}|^2) \end{aligned} \tag{12}$$

Since $\boldsymbol{X}_1^a$ and $\boldsymbol{X}_2^a$ are two distinct subsets of $\boldsymbol{X}^a$, it is not possible to have $x_{1,1} = \hat{x}_{1,1}$ and $x_{2,1} = \hat{x}_{2,1}$ concurrently. Therefore $\delta \neq 0$ for all values of $\boldsymbol{X}$ and $\hat{\boldsymbol{X}}$, and the corresponding PEP values can be calculated from (7), with $r = 3$. Once the PEP is calculated, the BEP of our scheme can be evaluated easily from (8).

In the case of the error events with higher lengths ($N \geq 3$), we can show that the diversity order of the 2-state code is again equal to 3, since the diverging and merging branch pairs for such error events correspond to a suberror event with $N = 2$, which we examined above. Assume that we have $\boldsymbol{X} = [\boldsymbol{X}(1)^{\mathrm{T}} \ldots \boldsymbol{X}(N)^{\mathrm{T}}]^{\mathrm{T}}$ and $\hat{\boldsymbol{X}} = [\hat{\boldsymbol{X}}(1)^{\mathrm{T}} \cdots \hat{\boldsymbol{X}}(N)^{\mathrm{T}}]^{\mathrm{T}}$ matrices with dimensions $2N \times 3$, where $\boldsymbol{X}(t)$ and $\hat{\boldsymbol{X}}(t)$ represent the transmitted and erroneously detected STBC-SM matrices, respectively, at the tth step of the error event. We have the expression given in (13), where $\boldsymbol{A}_1 = \boldsymbol{A}(\boldsymbol{X}(1), \hat{\boldsymbol{X}}(1)) + \boldsymbol{A}(\boldsymbol{X}(N), \hat{\boldsymbol{X}}(N))$ is the difference matrix for $N = 2$ and $\boldsymbol{A}_2 = \boldsymbol{A}(\boldsymbol{X}(2), \hat{\boldsymbol{X}}(2)) + \cdots + \boldsymbol{A}(\boldsymbol{X}(N-1), \hat{\boldsymbol{X}}(N-1))$. We know from Weyl's Theorem [18] that for the eigenvalues of the sum of two Hermitian matrices such as $\boldsymbol{A}_1$ and $\boldsymbol{A}_2$

$$\lambda_1(\boldsymbol{A}_1) + \lambda_1(\boldsymbol{A}_2) \leq \lambda_1(\boldsymbol{A}_1 + \boldsymbol{A}_2) \tag{14}$$

where $\lambda_1(\boldsymbol{A})$ denotes the smallest eigenvalue of $\boldsymbol{A}$. In our previous analysis, we have proved that $\mathrm{rank}(\boldsymbol{A}_1) = 3$, which implies that $\lambda_1(\boldsymbol{A}_1) \neq 0$. Consequently, $\mathrm{rank}(\boldsymbol{A}_1 + \boldsymbol{A}_2) = 3$, since $\lambda_1(\boldsymbol{A}_1 + \boldsymbol{A}_2) \neq 0$ regardless of $\lambda_1(\boldsymbol{A}_2)$. Therefore the diversity order of our scheme remains unchanged for higher values of N.

Similar analyses can be carried out easily for other code constructions. By generalising the concepts developed, here, we give the following remark:

Remark 1: The minimum CGD of the SOTC-SM scheme is always determined by parallel transitions and the error events with higher path lengths contribute higher diversity orders, which improve the distance spectrum of the proposed codes significantly. However, for the SOSTTCs with two transmit antennas, one has to consider error events with higher path lengths and their effect on the minimum CGD and more importantly, on the distance spectrum of the code. Therefore when compared with SOSTTCs, our scheme provides a much better distance spectrum, mainly because of the fact that the STBC-SM codewords are employed at the branches of the trellis and a systematic code design ensures higher diversity orders for $N > 1$ although the effects of parallel transitions are identical for both schemes.

4 Simplified ML decoding of SOTC-SM

In this section, we describe a simplified ML decoding technique for the SOTC-SM scheme and then compare its decoding complexity with that of SOSTTCs and SM-TC schemes. For the sake of simplicity, one receive antenna is assumed. However, a generalisation to multiple receive antennas is straightforward.

The encoding and decoding operations performed for the SOTC-SM scheme are as follows. For κ bits/s/Hz transmission, during each two consecutive symbol intervals, 2κ bits enter the SOTC-SM transmitter and determine the corresponding transition out of $2^{2\kappa}$ transitions on the trellis diverging from a given state. Each transition corresponds to the transmission of two symbols x_1 and x_2 in two consecutive symbol intervals from pairwise combinations of the available transmit antennas. The received signal samples during two time intervals can be expressed as $\boldsymbol{y} = \boldsymbol{X}\boldsymbol{h} + \boldsymbol{w}$, where $\boldsymbol{y} = [y_1 \ y_2]^{\mathrm{T}}$ and $\boldsymbol{w} = [w_1 \ w_2]^{\mathrm{T}}$ with w_i, $i = 1, 2$ being the additive Gaussian noise samples. $\boldsymbol{X}$ is the $2 \times n_T$ transmitted matrix, and $\boldsymbol{h} = \begin{bmatrix} h_1 & h_2 & \cdots & h_{n_T} \end{bmatrix}^{\mathrm{T}}$ is the $n_T \times 1$ channel vector, which is assumed to be perfectly known at the receiver, h_i representing the channel fading coefficient from the ith transmit antenna to the receiver. Similar to SOSTTCs, STTCs and SM-TC schemes, the Viterbi decoder, which decides on the most likely transmitted path, is used for ML decoding of the new scheme. The most likely transition with the minimum branch metric should be found among all parallel transitions at each state step of the Viterbi decoder for each state transition. For SOSTTCs, an approach is presented in [7] to reduce the total number of metric calculations, which benefits from the orthogonality of the core STBC by considering the subsets of orthogonal matrices for which a

$$\begin{aligned} \delta &= \det\begin{bmatrix} (\boldsymbol{X}(1) - \hat{\boldsymbol{X}}(1))^{\mathrm{H}} & \cdots & (\boldsymbol{X}(N) - \hat{\boldsymbol{X}}(N))^{\mathrm{H}} \end{bmatrix} \begin{bmatrix} (\boldsymbol{X}(1) - \hat{\boldsymbol{X}}(1)) \\ \vdots \\ (\boldsymbol{X}(N) - \hat{\boldsymbol{X}}(N)) \end{bmatrix} \\ &= \det[\boldsymbol{A}(\boldsymbol{X}(1), \hat{\boldsymbol{X}}(1)) + \boldsymbol{A}(\boldsymbol{X}(2), \hat{\boldsymbol{X}}(2)) + \cdots + \boldsymbol{A}(\boldsymbol{X}(N), \hat{\boldsymbol{X}}(N))] \\ &= \det[\boldsymbol{A}_1 + \boldsymbol{A}_2] \end{aligned} \tag{13}$$

separate decoding of x_1 and x_2 is applicable. Since we use the same set partitioning rules as those of SOSTTCs, a similar ML decoding technique can be used. From the received signals, the decoder can extract the embedded information symbol vector as

$$\boldsymbol{y}_{\text{eq}} = \mathcal{H}^m \boldsymbol{x} + \boldsymbol{w}_{\text{eq}} \tag{15}$$

where $\boldsymbol{x} = [x_1\ x_2]^{\text{T}}$. $\boldsymbol{y}_{\text{eq}} = \begin{bmatrix} y_1 & y_2^* \end{bmatrix}^{\text{T}}$ and $\boldsymbol{w}_{\text{eq}} = \begin{bmatrix} w_1 & w_2^* \end{bmatrix}^{\text{T}}$ are the equivalent received signal and noise vectors, respectively. $\mathcal{H}^m = \begin{bmatrix} \boldsymbol{h}_1^m & \boldsymbol{h}_2^m \end{bmatrix} = \begin{bmatrix} h_u & h_v \\ h_v^* & -h_u^* \end{bmatrix}$, $u, v \in \{1, 2, \ldots, n_T\}$ is the equivalent channel matrix [19] for the SOTC-SM scheme, where $\boldsymbol{h}_1^m = \begin{bmatrix} h_u & h_v^* \end{bmatrix}^{\text{T}}$, $\boldsymbol{h}_2^m = [h_v\ -h_u^*]^{\text{T}}$ and the index $m \in \{a, b, c, \ldots\}$ determines the corresponding antenna combination. As an example, for $\boldsymbol{X}^a$ and $\boldsymbol{X}^b$ given in (1), $u = 1$, $v = 2$ and $u = 2$, $v = 3$, respectively. Owing to the orthogonality ($(\boldsymbol{h}_1^m)^{\text{H}} \boldsymbol{h}_2^m = 0$, for all m), the decision metric $M_i^m(x_i)$ for x_i, $i = 1, 2$ can be separated as [20]

$$M_i^m(x_i) = \|\boldsymbol{y}_{\text{eq}} - \boldsymbol{h}_i^m x_i\|^2 \tag{16}$$

which reduces to the following for M-PSK by removing the constant terms after expansion

$$\begin{aligned} M_1^m(x_1) &= -\Re\{[y_1^* h_u + y_2\, h_v^*] x_1\} \\ M_2^m(x_2) &= \Re\{[y_2\, h_u^* - y_1^* h_v] x_2\} \end{aligned} \tag{17}$$

For simplified decoding, similar to SOSTTCs, we have to consider the subsets in which the metrics in (16) can be minimised independently. Furthermore, by calculating $M_1^m(x_1)$ and $M_2^m(x_2)$ for all values of x_1 and x_2, as well as saving the corresponding metrics, and using them for different subsets of the same partitioning level, the complexity of the decoder can be reduced significantly. The following example illustrates the simplified ML decoding of the SOTC-SM scheme:

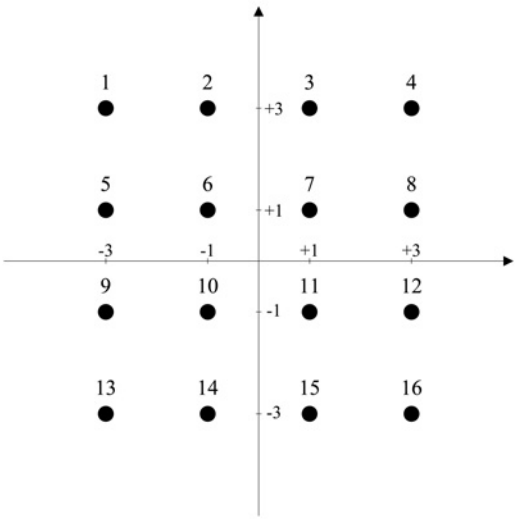

Fig. 3 *16-QAM constellation with corresponding symbol indices*

4.1 Example 4.1, (4 bits/s/Hz, 4-states)

For the new code given in Fig. 2, with a 16-QAM constellation, 256 different orthogonal matrices are assigned to each state of the trellis and the number of parallel transitions is 64. Without any simplification, the required number of metric calculations performed by the Viterbi decoder will be 256 per state, which is unacceptably high. However, considering that four distinct subsets ($\boldsymbol{X}_{11}$, $\boldsymbol{X}_{12}$, $\boldsymbol{X}_{21}$, $\boldsymbol{X}_{22}$) are assigned to the four parallel transitions from each state of the trellis, respectively, ML decoding can be simplified as follows. Let us define 16-QAM symbol sets $\mathcal{S}_1 = \{1, 3, 6, 8, 9, 11, 14, 16\}$ and $\mathcal{S}_2 = \{2, 4, 5, 7, 10, 12, 13, 15\}$ using the 16-QAM symbol indices given in Fig. 3. Then we have $(x_1, x_2) \in \mathcal{S}_1$, $(x_1, x_2) \in \mathcal{S}_2$, $x_1 \in \mathcal{S}_1$ and $x_2 \in \mathcal{S}_2$, and $x_1 \in \mathcal{S}_2$ and $x_2 \in \mathcal{S}_1$ for $\boldsymbol{X}_{11}^m$, $\boldsymbol{X}_{12}^m$, $\boldsymbol{X}_{21}^m$, and $\boldsymbol{X}_{22}^m$, respectively, where $m \in \{a, b, c, d\}$. As an example, to determine the parallel branch with the minimum metric in $\boldsymbol{X}_{11}^a$, the decoder minimises independently $M_1^a(x_1)$ and $M_2^a(x_2)$ over $x_1 \in \mathcal{S}_1$ and $x_2 \in \mathcal{S}_1$, respectively, and obtains the minimum branch metric as $M_1^a(\hat{x}_1^1) + M_2^a(\hat{x}_2^1)$, where $\hat{x}_i^j = \arg\min_{x_j \in \mathcal{S}_j} M_i^a(x_i)$ for $i, j = 1, 2$. Similarly, to determine the parallel branch with the minimum metric in $\boldsymbol{X}_{12}^a$, the decoder minimises independently $M_1^a(x_1)$ and $M_2^a(x_2)$ over $x_1 \in \mathcal{S}_2$ and $x_2 \in \mathcal{S}_2$, respectively, and obtains the corresponding minimum branch metric as $M_1^a(\hat{x}_1^2) + M_2^a(\hat{x}_2^2)$. These four minimisations require only 32 metric calculations in total. On the other hand, to determine the parallel branch having the minimum metric in $\boldsymbol{X}_{21}^a$ and $\boldsymbol{X}_{22}^a$, the decoder does not require new metric calculations. It just combines the previous minimum metrics as $M_1^a(\hat{x}_1^1) + M_2^a(\hat{x}_2^2)$ and $M_1^a(\hat{x}_1^2) + M_2^a(\hat{x}_2^1)$ for $\boldsymbol{X}_{21}^a$ and $\boldsymbol{X}_{22}^a$, respectively. The same procedure is applied for all antenna combinations.

In the above example, the subsets assigned to parallel transitions provide independent pairs for the calculation of (16). On the other hand, for some trellis codes, the subsets assigned to parallel transitions should be divided into smaller subsets to apply (16) for independent x_1 and x_2 pairs. As an example, for the 2-state SOTC-SM scheme, the same metrics as those of the 4-state SOTC-SM scheme should be calculated. However, the minimum branch metrics are calculated as $\min\{M_1^m(\hat{x}_1^1) + M_2^m(\hat{x}_2^1),\ M_1^m(\hat{x}_1^2) + M_2^m(\hat{x}_2^2)\}$ and $\min\{M_1^m(\hat{x}_1^1) + M_2^m(\hat{x}_2^2),\ M_1^m(\hat{x}_1^2) + M_2^m(\hat{x}_2^1)\}$ for $\boldsymbol{X}_1^m$ and $\boldsymbol{X}_2^m$, respectively, since $\boldsymbol{X}_1^m = \boldsymbol{X}_{11}^m \cup \boldsymbol{X}_{12}^m$ and $\boldsymbol{X}_2^m = \boldsymbol{X}_{21}^m \cup \boldsymbol{X}_{22}^m$. Similarly, for the 8-state-II SOTC-SM scheme, (16) cannot be applied directly, and consequently smaller subsets must be considered.

We observe that the total number of metric calculations performed at each step of the Viterbi decoder is the same for the SOTC-SM schemes and SOSTTCs given that both use the same trellis structure. However, the total number of operations performed can vary for the two systems depending on the considered signal constellation, as well as the trellis structure, if we save the common terms in (17) to reduce complexity. Using an approach similar to that in [7, Example 7.4.1], the following formula is derived to determine the total number of operations to be performed at each branch metric calculation step of the SOTC-SM Viterbi decoder, for our trellis codes constructed by the first technique using M-PSK

$$\begin{aligned} \xi = {} & \mathcal{O}(8n_T + 8SM - 24S) \\ & + \mathcal{O}(4n_T + 4SM - 12S + \mathcal{I}z) \end{aligned} \tag{18}$$

doi: 10.1049/iet-com.2012.0355

Table 2 Complexity comparison for different schemes

	2 bits/s/Hz (QPSK)			3 bits/s/Hz (8-PSK)		
	2-state	4-state	8-state	2-state	4-state	8-state
SM-TC	–	44 RM 28 RA	44 RM 28 RA	–	–	216 RM 152 RA
SOSTTC	32RM 24RA	32RM 24RA	–	96RM 56RA	184RM 104RA	376RM 216RA
SOTC-SM	40RM 28RA	64RM 48RA	104RM 180RA[a]	104RM 60RA	192RM 112RA	360RM 308RA[a]

[a]These values correspond to the complexity of the 8-state-II code, whereas the complexity of the 8-state-I code is the same as that of the 4-state code. On the other hand, the complexity of the 8-state-III code is only 8 RM + 4 RA higher than that of the 8-state-II code

where $\mathcal{O}(\cdot)$ notation is used to express the worst-case order of growth of the complexity, and the first and second terms in (18) correspond to the complexity of the real multiplications (RMs) and the real additions (RAs), respectively, S is the total number of different antenna combinations (or number of trellis states), z is the total number of different subsets assigned to the parallel transitions of the corresponding trellis, and $\mathcal{I} = 2$ for the 2- and 8-state SOTC-SM schemes, whereas $\mathcal{I} = 1$ for the 4-state SOTC-SM scheme. In Table 2, we present the total number of required operations for simplified decoding of SM-TC [16], SOSTTC [7] and the proposed SOTC-SM schemes with different trellis states using QPSK and 8-PSK constellations, in which the common terms are computed and saved for the reference schemes to reduce complexity. In general, we observe that the computational complexity of SOSTTCs is slightly lower than that of SOTC-SM when both schemes have the same trellis structure as seen from the first, fourth and fifth columns of Table 2. We also observe that, for the same trellis structure, the complexity of SM-TC for 3 bits/s/Hz is considerably lower than that of our SOTC-SM scheme; however, it requires a larger number of transmit antennas.

5 Simulation results and comparisons

In this section, computer simulation results are presented for the SOTC-SM scheme with different configurations and the error performance of the new scheme is compared with that of SOSTTCs and SM-TC schemes. BER and FER performance of these schemes was evaluated through Monte Carlo simulations for various spectral efficiencies and numbers of trellis states as a function of the average SNR per receive antenna. In all cases, the frame length is assumed to be 40κ bits for a spectral efficiency of κ bits/s/Hz. As it is not possible to use the same number of transmit antennas for all schemes, we make our comparisons based on the same spectral efficiency.

In Figs. 4 and 5, we compare the theoretical BEP approximations calculated in Section 3 with the computer simulation results, for the 2- and 4-state SOTC-SM schemes at 2 bits/s/Hz, respectively. As seen from these figures, for the error events with length $N = 2$, thanks to the SM, a transmit diversity order of three is obtained, as proven in Section 3. We also observe that the combined ($N = 1$ and 2) BEP converges to the BEP of the error events with $N = 1$, because of the improved distance spectrum of the

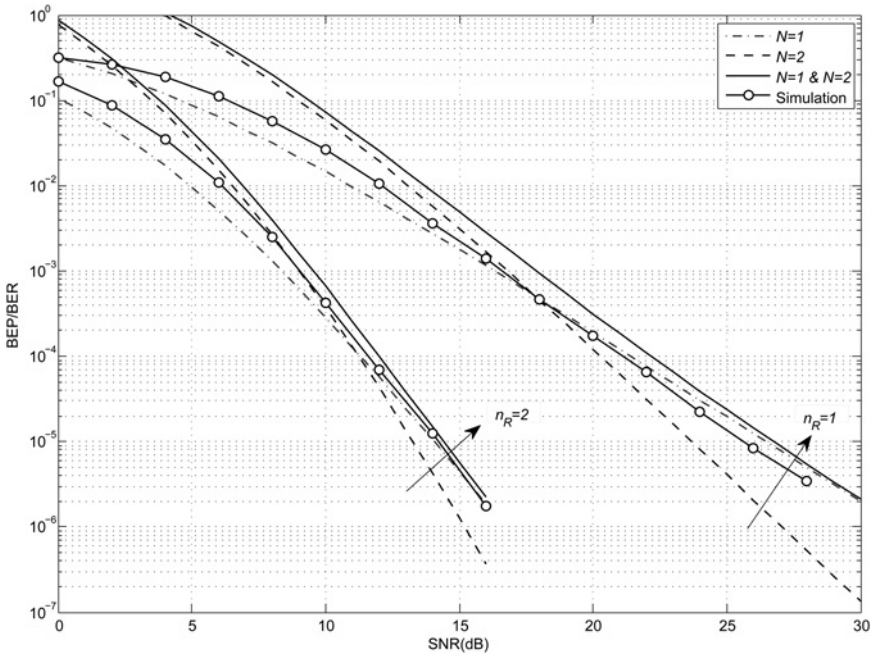

Fig. 4 *Comparison of theoretical BEP curves with simulation results for the 2-state SOTC-SM scheme at 2 bits/s/Hz, $n_T = 3$*

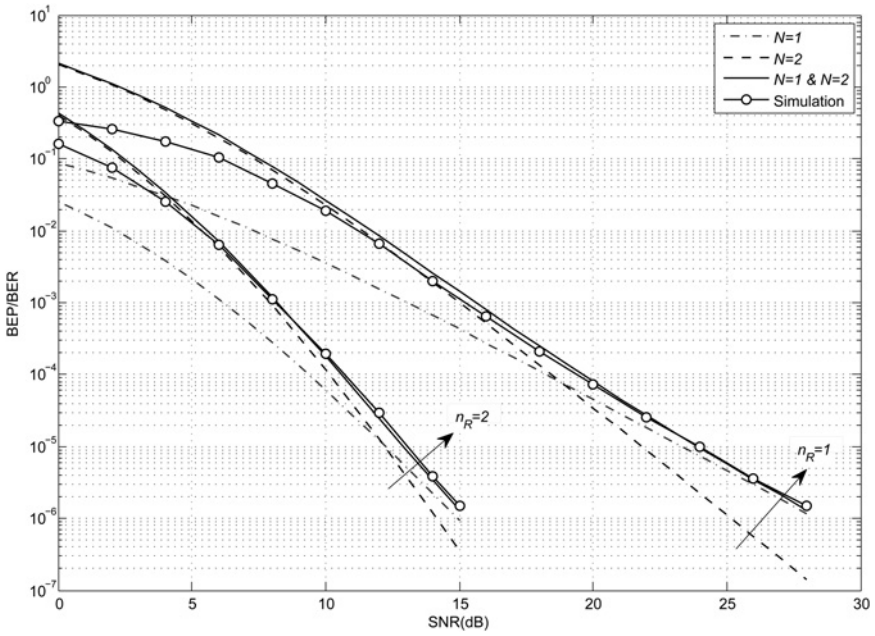

Fig. 5 *Comparison of theoretical BEP curves with simulation results for the 4-state SOTC-SM scheme at 2 bits/s/Hz, $n_T = 3$*

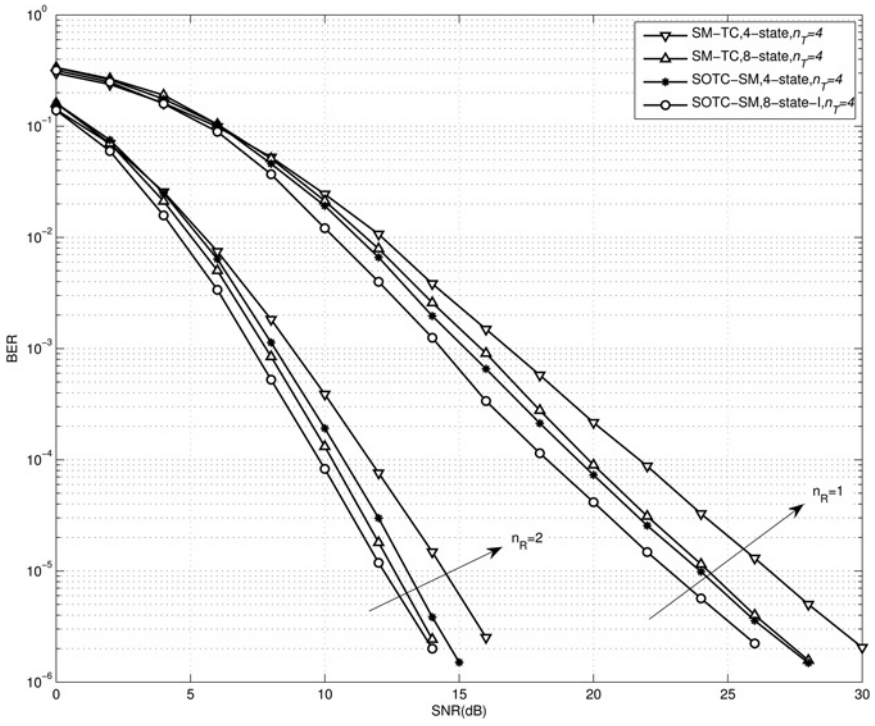

Fig. 6 *BER performance for 4- and 8-state SOTC-SM and SM-TC schemes at 2 bits/s/Hz*

proposed scheme. We also conclude that the given BEP approximations provide reasonably accurate results with increasing SNR and can be used to predict the error performance of the SOTC-SM scheme.

The BER performance of the SOTC-SM schemes with 2, 4 and 8 states is presented for 2 bits/s/Hz in Fig. 6. For comparison, we also depicted the BER performance of 4- and 8-state SM-TC schemes in Fig. 6. As seen from Fig. 6, a considerable improvement is achieved by the new schemes compared to the SM-TC schemes using same number of transmit antennas. We observe that the 4-state SOTC-SM scheme provides SNR gains of 2.6 and 1.3 dB over the 4-state SM-TC scheme for $n_R = 1$ and 2, respectively, whereas the 8-state SOTC-SM scheme provides SNR gains of 1.5 and 0.4 dB over the 8-state SM-TC scheme for $n_R = 1$ and 2, respectively.

The FER performance of the SOTC-SM schemes with 2, 4 and 8 states is presented for 2 bits/s/Hz in Fig. 7. As seen from

doi: 10.1049/iet-com.2012.0355

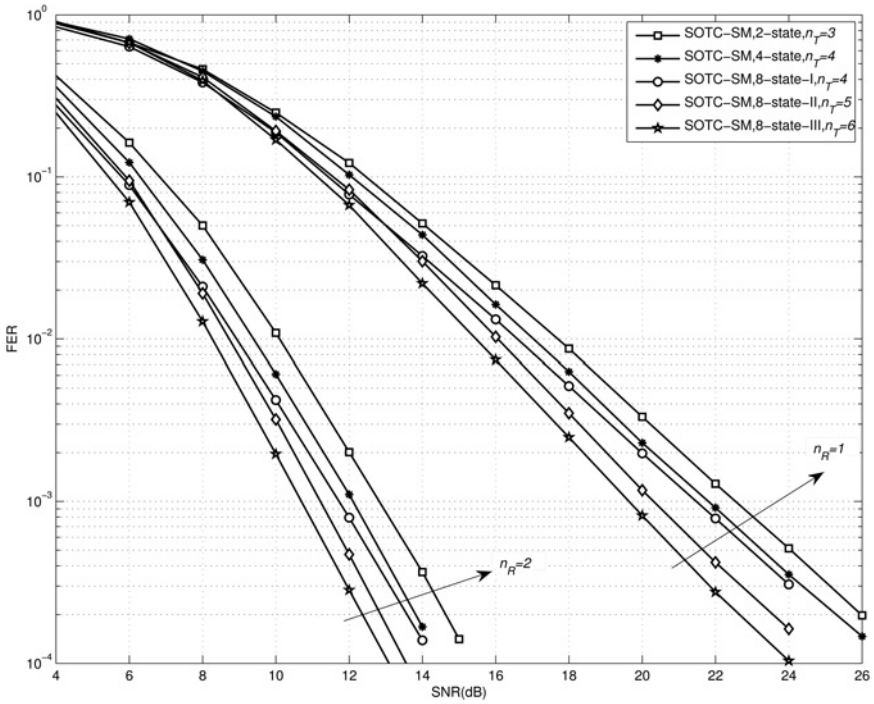

Fig. 7 *FER performance for 2-, 4- and 8-state SOTC-SM schemes at 2 bits/s/Hz*

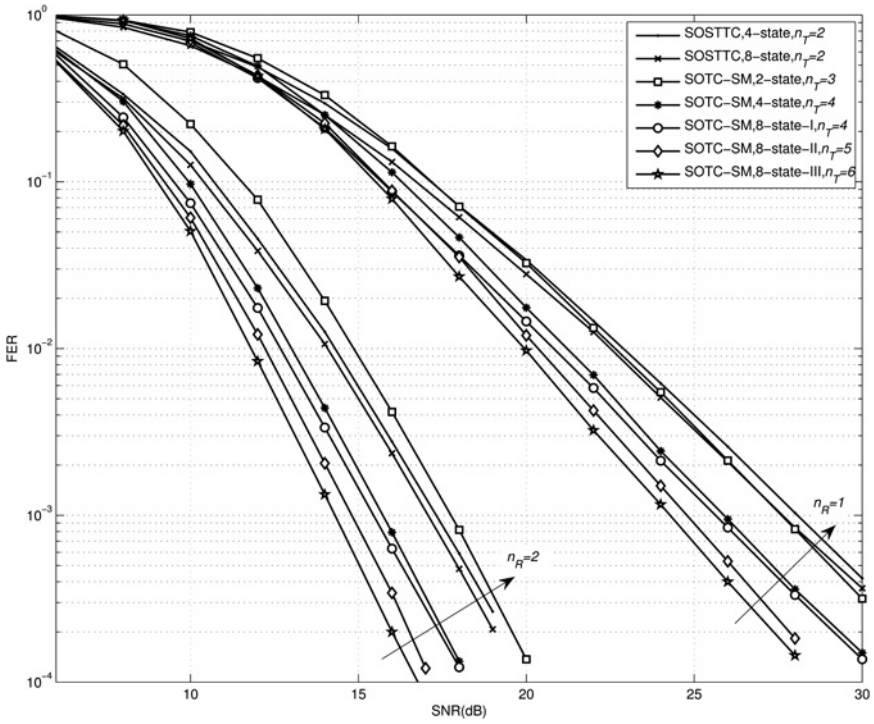

Fig. 8 *FER performance for 2-, 4- and 8-state SOTC-SM, SOSTTC and schemes at 3 bits/s/Hz*

Fig. 7, the SOTC-SM technique exhibits improved FER performance by increasing number of transmit antennas. As an example, for $n_R = 1$, because of its improved distance spectrum, the 8-state-III SOTC-SM scheme provides SNR gains of 0.7, 1.9, 2.2, and 3.0 dB over the 8-state-II, 8-state-I, 4-state and 2-state SOTC-SM schemes, respectively.

In Fig. 8, the FER performance of the SOTC-SM schemes is given for 3 bits/s/Hz. For comparison, the FER performance of the 4- and 8-state SOSTTCs are also given in the same figure. Although exploiting larger number of transmit antennas than the SOSTTCs, our proposed codes achieve significantly better FER performance than the SOSTTCs by using the same number of RF chains at the transmitter since only two transmit antennas remain active in our scheme during transmission. As an example, the 4-state SOTC-SM provides SNR gains of 2.2 and 1.6 dB over the 4-state SOSTTC for $n_R = 1$ and 2, respectively, whereas the 8-state-I SOTC-SM provides SNR gains of 2.1 and 1.7 dB over the 8-state SOSTTC for $n_R = 1$ and 2, respectively. On the other hand, 8-state-III and 8-state-II

codes exhibit improved FER performance compared with the 8-state-I code because of their better distance spectra.

6 Conclusions

In this paper, we have introduced a novel coded-MIMO scheme called SOTC-SM as an alternative to SOSTTCs and SM-TC schemes given in the literature. Systematic techniques have been presented to construct the new scheme for a given spectral efficiency and number of trellis states. The BEP performance of the proposed scheme has been investigated by performing a detailed PEP analysis. A simplified ML detection technique has been provided to reduce the decoding complexity of the SOTC-SM scheme. It has been shown through computer simulations that the proposed SOTC-SM schemes achieve significantly better error performance than SOSTTCs and SM-TC with a comparable decoding complexity.

7 Acknowledgments

Ertuğrul Başar acknowledges the support of The Scientific and Technological Research Council of Turkey (TÜBİTAK) of his position within the Department of Electrical Engineering, Princeton University.

8 References

1 Wolniansky, P., Foschini, G., Golden, G., Valenzuela, R.: 'V-BLAST: an architecture for realizing very high data rates over the rich-scattering wireless channel'. Proc. Int. Symp. Signals, Systems, Electronics (ISSSE98), Pisa, Italy, September 1998, pp. 295–300

2 Alamouti, S.: 'A simple transmit diversity technique for wireless communications', *IEEE J. Sel. Areas Commun.*, 1998, **16**, (8), pp. 1451–1458

3 Tarokh, V., Jafarkhani, H., Calderbank, A.: 'Space-time block codes from orthogonal designs', *IEEE Trans. Inf. Theory*, 1999, **45**, (5), pp. 1456–1467

4 Tarokh, V., Seshadri, N., Calderbank, A.: 'Space-time codes for high data rate wireless communication: performance criterion and code construction', *IEEE Trans. Inf. Theory*, 1998, **44**, (2), pp. 744–765

5 Ungerboeck, G.: 'Channel coding with multilevel/phase signals', *IEEE Trans. Inf. Theory*, 1982, **28**, (1), pp. 55–67

6 Jafarkhani, H., Seshadri, N.: 'Super-orthogonal space-time trellis codes', *IEEE Trans. Inf. Theory*, 2003, **49**, (4), pp. 937–950

7 Jafarkhani, H.: 'Space-time coding' (Cambridge University Press, 2005)

8 Mesleh, R., Haas, H., Sinanovic, S., Ahn, C.W., Yun, S.: 'Spatial modulation', *IEEE Trans. Veh. Technol.*, 2008, **57**, (4), pp. 2228–2241

9 Jeganathan, J., Ghrayeb, A., Szczecinski, L., Ceron, A.: 'Space shift keying modulation for MIMO channels', *IEEE Trans. Wirel. Commun.*, 2009, **8**, (7), pp. 3692–3703

10 Renzo, M.D., Haas, H.: 'Space shift keying (SSK-) MIMO over correlated rician fading channels: Performance analysis and a new method for transmit-diversity', *IEEE Trans. Commun.*, 2011, **59**, (1), pp. 116–129

11 Sugiura, S., Chen, S., Hanzo, L.: 'Coherent and differential space-time shift keying: A dispersion matrix approach', *IEEE Trans. Commun.*, 2010, **58**, (11), pp. 3219–3230

12 Yang, P., Xiao, Y., Yu, Y., Li, S.: 'Adaptive spatial modulation for wireless MIMO transmission systems', *IEEE Commun. Lett.*, 2011, **15**, (6), pp. 602–604

13 Wang, J., Jia, S., Song, J.: 'Signal vector based detection scheme for spatial modulation', *IEEE Commun. Lett.*, 2012, **16**, (1), pp. 19–21

14 Başar, E., Aygölü, Ü., Panayirci, E., Poor, H.V.: 'Space-time block coded spatial modulation', *IEEE Trans. Commun.*, 2011, **59**, (3), pp. 823–832

15 Mesleh, R., Renzo, M.D., Haas, H., Grant, P.M.: 'Trellis coded spatial modulation', *IEEE Trans. Wirel. Commun.*, 2010, **9**, (7), pp. 2349–2361

16 Başar, E., Aygölü, Ü., Panayirci, E., Poor, H.V.: 'New trellis code design for spatial modulation', *IEEE Trans. Wirel. Commun.*, 2011, **10**, (9), pp. 2670–2680

17 Simon, M., Alaouni, M.S.: 'Digital communications over fading channels' (John Wiley & Sons, 2005)

18 Horn, R.A., Johnson, C.R.: 'Matrix analysis' (Cambridge University Press, 1985)

19 Hassibi, B., Hochwald, B.: 'High-rate codes that are linear in space and time', *IEEE Trans. Inf. Theory*, 2002, **48**, (7), pp. 1804–1824

20 Guo, X., Xia, X.G.: 'On full diversity space-time block codes with partial interference cancellation group decoding', *IEEE Trans. Inf. Theory*, 2009, **55**, (10), pp. 4366–4385

doi: 10.1049/iet-com.2012.0355